6-27-2018

Two-Dimensional Crystallization of Poly(N-isopropylacrylamide)-Capped Gold Nanoparticles

Wenjie Wang
Ames Laboratory, wenjiew@ameslab.gov

Jack J. Lawrence
Ames Laboratory

Wei Bu
University of Chicago

Honghu Zhang
Iowa State University and Ames Laboratory

David Vaknin
Ames Laboratory, vaknin@ameslab.gov

Two-Dimensional Crystallization of Poly(N-isopropylacrylamide)-Capped Gold Nanoparticles

Abstract
Surface-sensitive X-ray reflectivity and grazing incidence small-angle X-ray scattering reveal the structure of polymer-capped-gold nanoparticles (AuNPs that are grafted with poly(*N*-isopropylacrylamide); PNIPAM–AuNPs) as they self-assemble and crystallize at the aqueous suspension/vapor interface. Citrate-stabilized AuNPs (5 and 10 nm in nominal diameter) are ligand-exchanged by 6 kDa PNIPAM-thiol to form corona brushes around the AuNPs that are highly stable and dispersed in aqueous suspensions. Surprisingly, no clear evidence of thermosensitive effect on surface enrichment or self-assembly of the PNIPAM–AuNPs is observed in the 10–35 °C temperature range. However, addition of simple salts (in this case, NaCl) to the suspension induces migration of the PNIPAM–AuNPs to the aqueous surface, and above a threshold salt concentration, two-dimensional crystals are formed. The 10 nm PNIPAM–AuNPs form a highly ordered single layer with in-plane triangular structure, whereas the 5 nm capped NPs form short-range triangular structure that gradually becomes denser as salt concentration increases.

Disciplines
Engineering Physics | Metallurgy | Nanoscience and Nanotechnology

Two-Dimensional Crystallization of Poly(N-isopropylacrylamide)-Capped Gold Nanoparticles

Wenjie Wang,[†] Jack J. Lawrence,[†] Wei Bu,[‡] Honghu Zhang,[¶] and David Vaknin[*,§]

†*Division of Materials Sciences and Engineering, Ames Laboratory, USDOE, Ames, Iowa 50011, United States*

‡*NSF's ChemMatCARS, University of Chicago, Illinois 60637, United States*

¶*Ames Laboratory, and Department of Materials Science and Engineering, Iowa State University, Ames, Iowa 50011, United States*

§*Ames Laboratory, and Department of Physics and Astronomy, Iowa State University, Ames, Iowa 50011, United States*

E-mail: vaknin@ameslab.gov

Abstract

Surface sensitive X-ray reflectivity (XR) and grazing incidence small angle X-ray scattering (GI-SAXS) reveal the structure of polymer-capped-gold nanoparticles (AuNPs that are grafted with Poly(N-isopropylacrylamide ; PNIPAM-AuNPs) as they self-assemble and crystallize at the aqueous-suspension/vapor interface. Citrate stabilized AuNPs (5 and 10 nm in nominal diameter) are ligand-exchanged by 6 kDa PNIPAM-thiol to form corona brushes around the AuNPs that are highly stable and dispersed in aqueous suspensions. Surprisingly, no clear evidence of thermosensitive

effect on surface enrichment or self-assembly of the PNIPAM-AuNPs is observed in the 10 to 35 °C temperature range. However, addition of simple salts (in this case, NaCl) to the suspension induces migration of the PNIPAM-AuNPs to the aqueous surface, and above a threshold salt concentration, two dimensional crystals are formed. The 10 nm PNIPAM-AuNPs form a highly ordered single-layer with in-plane triangular structure, whereas the 5 nm capped NPs form short range triangular structure that gradually becomes denser as salt concentration increases.

Introduction

Various non-ionic water-soluble polymers phase separate in response to the presence of salts in solution, to variations in pH or temperature and their combinations, and other stimuli (i.e., electric or magnetic field).[1–3] For instance, polyethylene-glycol (PEG) phase separates in the presence of various salts with a moderate dependence on temperature that varies with the salt species.[4,5] Poly(N-isopropylacrylamide) (PNIPAM) is a well known thermosensitive polymer exhibiting a reversible phase separation upon cycling temperature through the so called lower critical solution temperature ($T_{LCST} \approx 32$ °C).[3,6] It has also been shown that PNIPAM, in aqueous solution, like PEG, is responsive to sodium based salts by lowering the LCST in accordance with the anionic Hofmeister series.[7] The aqueous bi-phase phenomena of these non-ionic polymers has since been exploited for a variety of application most notably for isolating and concentrating biomaterials.[8,9] Recently, the bi-phasic separation has been been successfully used for self-assembly and crystallization of PEG capped nanoparticles at vapor-suspension interfaces by adjusting salt concentrations[10–13]. Furthermore, sufficiently high salt concentrations induce three dimensional crystalline precipitates as has been observed in small angle X-ray scattering studies.[14] Similarly, it has been demonstrated that PNIPAM-NH_2-AuNPs can form a mono-layer at water/oil interfaces such that their nearest-neighbor distance can be tuned by varying temperature, consequently leading to rapid switching of the optical properties of the mono-layer.[15] Grazing incidence small angle x-ray scattering

(GISAXS) experiments of silver-coated PNIPAM-C18 films, prepared by dropcast and drying on a Si waffer, show that superlattices are formed with a lattice constant that shrinks and expands reversibly in response to variation of relative humidity and to a lesser extent due to temperature changes.[16]

Here, we explore the response of PNIPAM brushes capping gold nanoparticles (PNIPAM-AuNPs) to salt (NaCl) in suspensions by determining the vapor/aqueous suspension structure (see schematic illustration in Fig. 1). We use surface sensitive synchrotron X-ray scattering techniques to determine the interfacial structure as has been demonstrated for DNA-AuNPs[17–20] and more recently for PEG-AuNPs suspensions in the presence of various salts.[10,11]

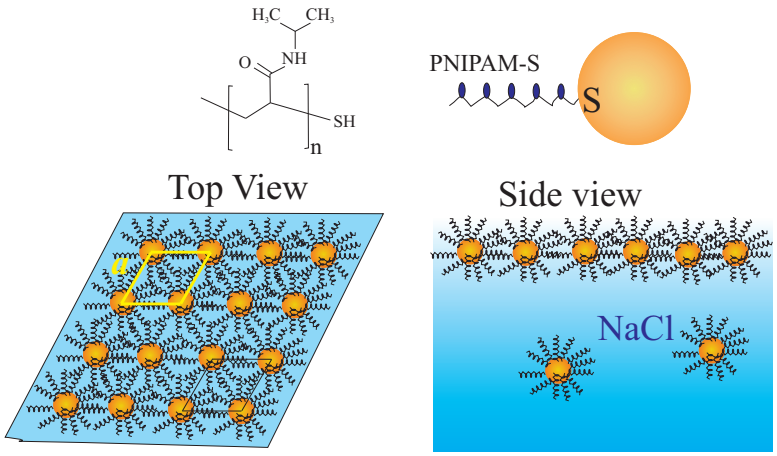

Figure 1: PNIPAM-S molecule bound to a AuNP and illustration of the effect of adding NaCl to PNIPAM-AuNPs suspension. A single densely packed mono-layer is formed at the suspension-vapor interface and GISAXS shows the assembled PNIPAM-AuNPs crystallize into high quality 2D triangular lattice.

Materials and Experimental setup

Commercial nominal 5 and 10 nm gold nanoparticles are purchased from Ted Pella already stabilized by citrates. Monothiol-terminated poly(N-isopropyl acrylamide) powder with molecular weight of 6 kDa is purchased from Sigma-Aldrich. The PNIPAM-thiol is dissolved in the 50% (v/v) ethanol aqueous solution before mixing with AuNPs. The ratio of PNIPAM-thiol needed to sufficiently react and cover the nanoparticles is estimated by the

surface area of a single 10 nm nanoparticle divided by the molecular area of a sulfur-gold bond that is assumed to be 0.2 nm^2. Experimentally, optimal functionalization is achieved by using an excess of PNIPAM-thiol by a factor of 4 from the calculated ratio; in our case, PNIPAM is mixed with the 10 nm gold nanoparticles at a ratio of 6000/1 moles of PNIPAM per mole of nanoparticles. The mixture is left to stir for 24 to 48 hours to ensure maximum loading. After stirring, the sample is transferred to 1.7 mL tubes and centrifuged. Upon centrifugation, the nanoparticles aggregate to the bottom of each tube and the supernatant is withdrawn and replaced with Millipore water. This process is repeated three times to remove citrates and excess PNIPAM not bound to the nanoparticles. Centrifugation can also be used to control the concentration of nanoparticle in the solution. The concentration of gold nanoparticles is determined by UV-vis analysis using an extinction coefficient provided by the Ted Pella website (at 520nm). The final concentrations of 10 and 5 nm AuNPs-PNIPAM used in the experiments were 12.5 and 42.1 nM.

Both X-ray reflectivity (XR) and grazing incident small X-ray angle scattering (GISAXS) measurements were carried out at ChemMatCARS (beamline ID-15) of the Advanced Photon Source (APS) at Argonne National Laboratory with incident X-ray energy of 10 keV. We used a liquid surface reflectometer, described in detail elsewhere,[23] for both XR and GISAXS. While the incident beam intensity is monitored by an ionization chamber, the outgoing beam intensities are recorded by a Pilatus 100K detector (Dectris). GISAXS data are obtained at the grazing incident angle 0.09° (below the critical angle for total reflection). The instrumental resolution of GISAXS is $\delta Q = 0.0008$ $Å^{-1}$, determined by the detector pixel size (0.172 mm) and the sample-to-detector distance (1065 mm). For the X-ray measurements, the PNIPAM-AuNPs suspension sample ($\sim$ 1.5 mL) is held in a stainless steel trough (approximate dimensions $20 \times 120 \times 0.3$ mm) that was enclosed in a thermostated chamber. The sample chamber is continuously purged with water-saturated helium (helium gas is bubbled through water prior to purging) to reduce background scattering and minimize radiation damage to the film. The stainless steel trough is placed on a thermostated

copper plate with capability to control the temperature of the chamber from about 10 to 60 °C. We have conducted XR and GISAXS experiments of the suspension as a function of temperature in the range of 10 to 35 °C that did not yield results that differed significantly from bare water interfaces. Thus, the results presented here are from PNIPAM-AuNPs in salt (NaCl) solutions and performed at room temperature i.e., 22 °C.

Results and Discussion

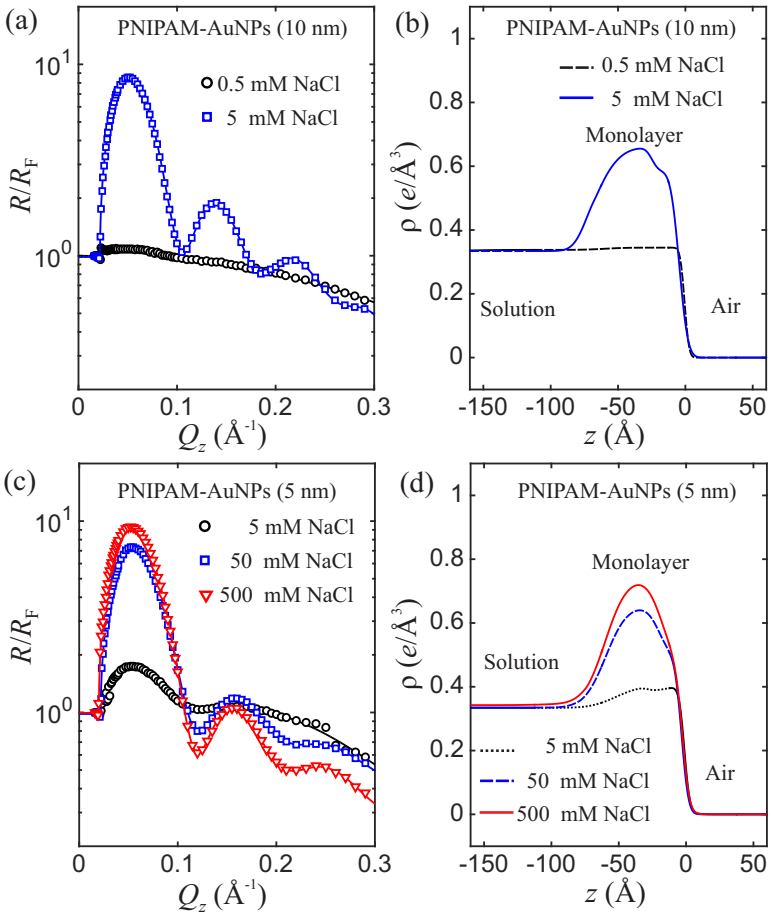

Figure 2: (a) Normalized X-ray reflectivity R/R_F (R_F is the reflectivity from ideally flat suspension interface, i.e., no surface roughness) from 12.5 nM PNIPAM-AuNPs suspension of nominal 10 nm Au core diameter at various NaCl concentrations as indicated. Solid lines are obtained from a best fit electron density (ED) model shown in (b) (c) R/R_F form 42.1 nM PNIPAM-AuNPs suspensions of nominal 5 nm Au core diameter at various NaCl concentrations as indicated. Solid lines of R/R_F are obtained from a best fit ED model shown in (d). Data were collected at room temperature.

Specular X-ray reflectivity (XR) as a function of momentum transfer along the surface normal (Q_z) is employed to yield the density profiles as a function of depth of nanoparticle-

films as they enrich the liquid/vapor interfaces.[10,11,17–20] Figure 2 (a) shows normalized reflectivity $R/R_{\rm F}$ data (R_F is the XR from an ideally flat solution surface) from surfaces of PNIPAM-AuNPs (AuNPs are 10 nm in diameter) suspensions in the presence of varying concentrations of NaCl. In the absence of salt in the PNIPAM-AuNPs suspensions, the XR is featureless falling off as $\exp\left(-Q_z^2\sigma^2\right)$ due to surface roughness (σ is a measure of the surface roughness), as is typically observed for a pure bare liquid/vapor interface. Similarly, at relatively low NaCl concentration (i.e., [NaCl]=0.5 mM), the $R/R_{\rm F}$ data curve shows monotonic decrease with a very weak feature compared to a bare surface solution, indicating the initiation of accumulated PNIPAM -AuNPs at the interface. However, at 5 mM NaCl, the $R/R_{\rm F}$ curve changes significantly by exhibiting evenly spaced interference pattern characteristic of a uniform film.[21,22] The separation of the consecutive maxima, ΔQ_z, is approximately 0.09 Å^{-1}, corresponding to an average thickness of $2\pi/\Delta Q_z \approx 70$ Å, dominated by the electron-density (ED) of AuNPs. Further increase in salt to the PNIPAM-AuNPs suspensions results in abrupt discontinuities in R/R_F indicating severe inhomogeneities at the interface due to precipitation of aggregates (data not shown). Detailed analysis of the XR, yields the corresponding ED profiles shown in Fig.2 (b). The ED profile corresponding to the low NaCl bulk concentration ([NaCl]=0.5 mM) resembles a smooth step-like function with a finite transition width ($\sigma \approx 4$ Å) from bulk ED to zero at the vapor–liquid interface located at $z \approx 0$. For [NaCl] = 5 mM, the ED enhanced region extends over ~ 100 Å and peaks at $z \approx -34$ Å with a full-width-at-half-maximum (FWHM) ≈ 6 nm with respect to the bulk ED. We note that the the ED of planar spherical particles with centers at $z = z_0$ varies along the surface normal, z-axis, proportional to $(D/2)^2 - (z - z_0)^2$, with a maximum ED at $z = z_0$ and a FWHM$= D/\sqrt{2}$. SAXS measurements of our bare AuNPs indicates the average size of the nominal diamter $D = 8.8(\pm 9\%)$ nm ($\pm$ sign indicates size distribution), yielding a FWHM ≈ 6 nm, in good agreement with the value extracted from the measured ED. This is also consistent with the surface ED profiles determined for aqueous surface superlattices of PEG-AuNPs that are induced by salts[10,12]. The asymmetry of the film ED

(different widths at the vapor and liquid interfaces) and a small step like at the film/gas interface suggest that the PNIPAM polymers around the AuNPs are at different states at the two interfaces, i.e., those close to the gas phase are highly compressed and concentrated while those in proximity of the fluid are loosely packed and extended into the subphase.[10,12] In general, we find that the ED of organic-polymers in aqueous medium is not significantly different that of the surrounding solution and therefore practically impossible to distinguish from the subphase in X-ray scattering experiments.[10,11]

Similar film formation is also obtained for the nominal size $D = 5$ nm PNIPAM-AuNPs as salt is added to the suspension, however, higher salt concentration is necessary to saturate the surface. Figure 2 (c) shows the normalized XR where interference features emerge at 5 mM NaCl. Here too, for [NaCl] below 5 mM, the R/R_{F} profiles resemble that of a bare liquid surface (data not shown). Further increase of bulk [NaCl] enhances the R/R_{F} maxima significantly, and for [NaCl] = 500 mM the surface is saturated with PNIPAM-AuNPs. Even though the R/R_{F} maxima increase upon the bulk [NaCl], the separation of the consecutive maxima, $\Delta Q_z \approx 0.11$ Å^{-1}, are evidence that the uniform slab consists of a single layer of PNIPAM-AuNPs with average thickness 57 Å, independent of bulk [NaCl]. The corresponding ED profiles shown in Fig. 2 (d) manifest similar features to those obtained in Fig. 2 (b), i.e., asymmetric ED enhanced region at the interface, with broader interface towards subphase and a FWHM≈ 45 Å. Our SAXS data shows that the nominal 5 nm AuNPs are in fact 6.5(±15%) nm in diameter which is consistent with the FWHM extracted from the ED. The XR results in Fig. 2 also show that it takes at least one order of magnitude more salt to bring the 5 nm AuNPs to the surface and give rise to the similar R/R_F maximum (or alternatively, the maximum ED) than that used for the 10 nm AuNPs. A qualitative explanation follows. Since the maximum XR or equivalently maximum ED is a measure of the maximum in-plane Au density, it takes more small-sized AuNPs to populate the surface to reach the same surface density of large-sized AuNPs. The aqueous surface affinity is driven by PNIPAM, and the larger AuNPs in general have more PNIPAM polymers grafted

on their surfaces than smaller AuNPs. Thus, the same salts concentration level drive more large-sized AuNPs to the aqueous surface than the small-sized AuNPs. Therefore, more salt is required to bring more small-sized AuNPs to populate the surface to reach comparable XR maximum (or ED maximum).

Whereas the XR results clearly demonstrate a nanoparticle mono-layer formation at the suspension/gas interfaces driven by bulk salt concentration, raising the temperature gradually (of PNIPAM-AuNPs without salt) from from 10 to about 35 °C (above the LCST $\approx$ 32 °C) does not show the slightest evidence of surface enrichment of PNIPAM-AuNPs due the bi-phasic behavior of PNIPAM. Below, we examine the in-plane structure of the PNIPAM-AuNPs in the film, by GISAXS method on the same samples that the XR are performed on.

GISAXS determines the lateral packing of the PNIPAM-AuNPs within a nanoparticle mono-layer at the interface observed in the XR studies described above. Figure 3 (a) shows the GISAXS intensity as a function of the in-plane momentum-transfer Q_{xy} (integrated over a finite range of Q_z values) for the 10 nm PNIPAM-AuNPs suspension at [NaCl] = 0.5 and 5 mM. At the low NaCl concentration, the practically undetected GISAXS signal is consistent with the XR results that show an almost bare surface. At the 5 mM NaCl concentration, strong Bragg reflections emerge with peak positions at $Q_{xy} = Q_i$ ($i = 1, 2, 3...$ that conform to the ratio $Q_i/Q_1 = 1, \sqrt{3}, \sqrt{4}, \sqrt{7}$ (see inset of Fig. 3), considering the most intense peak at $Q_{xy} = Q_1 = 0.0269$ Å^{-1} as the primary peak. These ratios correspond to a 2D triangular lattice, similar to surface crystallization of DNA-AuNPs[20] or PEG-AuNPs.[10,11] The lattice constant of the unit cell is $a = 4\pi/(\sqrt{3}Q_1) \approx 270$ Å.

The effect of salt on the surface assembly of PNIPAM-AuNPs with 5nm diameters cores is shown on Fig. 3 (b). At low salt concentration (below 5 mM) the pattern is void of any diffraction peaks. However, as the concentration is raised, two broad peaks are observed that shift to higher Q_{xy} values with the increase of salt concentration indicating shrinking nearest-neighbor distances. This is consistent with the gradual increase in surface density of

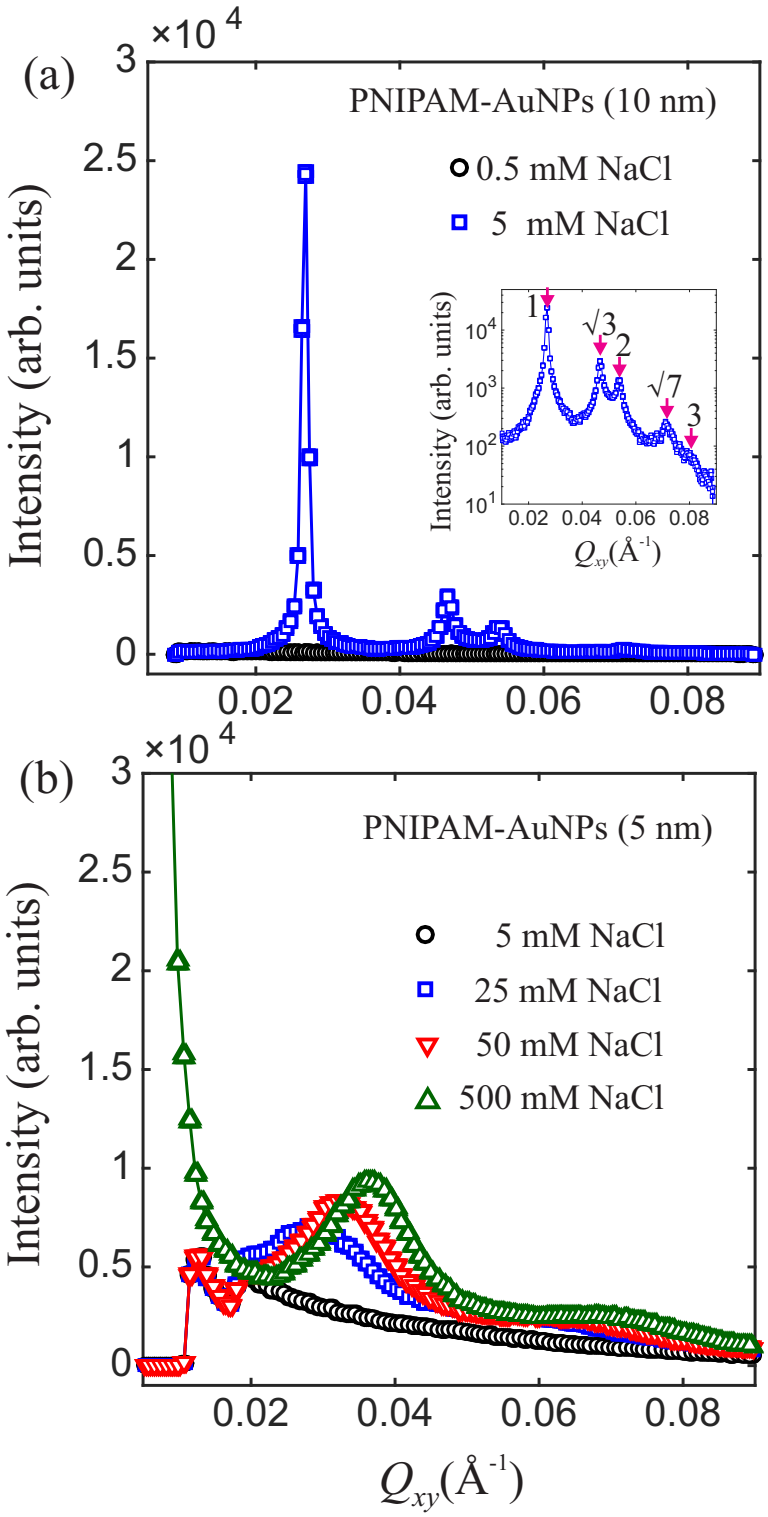

Figure 3: GISAXS as a function of inplane-momentum transfer Q_{xy} integrated over Q_z for PNIPAM-AuNP suspensions in the presence of NaCl at various concentrations as indicated. (a) Nominal AuNP diameter 10 nm at 12.5 nM. The inset shows the same diffraction pattern with intensities displayed on logarithmic scale with indexing Bragg reflections that correspond to 2D triangular lattice of PNIPAM-AuNPs at 5 mM NaCl.(b) Surface diffraction patterns from 5 nm AuNPs-PNIPAM (42.1 nM suspension) at various NaCl concentrations. Data were collected at room temperature.

PNIPAM-AuNPs at the interface as observed in the XR discussed above. The ratio between the position of the secondary peak to that of the primary $Q_1 \approx 0.036$ Å is $\approx \sqrt{3}$, indicating triangular ordering, albeit at short range order compared to the 10 nm PNIPAM-AuNPs ordering. The unit cell lattice constant at 500 mM NaCl is estimated at $a = 4\pi/(\sqrt{3}Q_1) \approx$ 201 Å.

Discussion and Conclusion

Using X-ray reflectivity (XR) from liquid suspensions of polymer-capped gold nanoparticles (AuNPs that are grafted with Poly(N-isopropylacrylamide); PNIPAM-AuNPs) we show that the addition of NaCl to the suspension induces the formation of a nanoparticle mono-layer at the gas/liquid interface. Furthermore, grazing incidence small angle X-ray scattering (GISAXS) measurements of the same films demonstrate that the self-assembled PNIPAM-AuNPs at the liquid/gas interface crystallize into triangular stable structures. Our primary goal in conducting this study, has been to look for reversible assembly and crystallization in response to temperature variation across the LCST ($T_{LCST} \approx 32$ °C of PNIPAM in aqueous solutions, above which phase separation occurs), but surprisingly, no evidence of thermosensitive effect on surface enrichment or self-assembly of the PNIPAM-AuNPs is observed in the 10 to 35 °C temperature range. This is consistent with a recent study by Turek et al. that demonstrates the crucial role played by salts (e.g., NaCl) in the suspensions of PNIPAM-AuNPs for forming bulk aggregates, i.e., salts bring about charge screening that facilitate nanopartcle aggregation.[24] That study also shows the salts are more effective in inducing the PNIPAM-AuNPs bulk assembly than elevating temperature, a fact consistent with our finding regarding to the aqueous surface assembly of the PNIPAM AuNPs. We show that moderate salt concentrations in 10 nm core diameter AuNPs PNIPAM-AuNPs induce a highly ordered single-layer with in-plane triangular structure, whereas for the 5 nm capped NPs form short range triangular structure that gradually becomes denser as salt

concentration increases.

Acknowledgements

We thank Mr. Talon Brown (Ames Laboratory) for experimental help in the initial stages of this work. Research was supported by the U.S. Department of Energy, Office of Basic Energy Sciences, Division of Materials Sciences and Engineering. Ames Laboratory is operated for the U.S. Department of Energy by Iowa State University under Contract No. DE-AC02-07CH11358. NSF's ChemMatCARS Sector 15 is principally supported by the Divisions of Chemistry (CHE) and Materials Research (DMR), National Science Foundation, under grant number NSF/CHE-1346572. Use of the Advanced Photon Source, an Office of Science User Facility operated for the U.S. Department of Energy (DOE) Office of Science by Argonne National Laboratory, was supported by the U.S. DOE under Contract No. DE-AC02-06CH11357.

References

(1) Bekturov, E. A. & Khamzamulina, R. E. Solution Properties of Water-Soluble Nonionic Polymers. J. Macromol. Sci. - Reviews in Macromolecular Chemistry and Physics, **1987**, *C27*, 253-312.

(2) Cabezas, Jr H.; Theory of Phase Formation in Aqueous Two-Phase Systems. *J. Chromatography B*, **1996**, *680* 3-30.

(3) Aseyev, V.; Tenhu, H.; and Winnik, F. M.; Non-ionic Thermoresponsive Polymers in Water. *Adv. Polym. Sci.*, **2011**, *242*, 29-89.

(4) Willauer, H. D.; Huddleston, J. G.; Rogers, R. D. Solute Partitioning in Aqueous Biphasic Systems Composed of Polyethylene Glycol and Salt: The Partitioning of Small Neutral Organic Species. *Ind. Eng. Chem. Res.* **2002**, *41*, 1892-1904.

(5) Huddleston, J. G.; Willauer, H. D.; Rogers, R. D. Phase Diagram Data for Several PEG + Salt Aqueous Biphasic Systems at 25 °C. *J. Chem. Eng. Data* **2003**, *48*, 1230-1236.

(6) Heskins. M.; Guillet, J. E. Solution Properties of Poly (N-isopropylacrylamide). *J. Macromol. SC1.-CHEM.*, **1968**, *A2(8)*, 1441-1455.

(7) Zhang, Y.; Furyk, S.; Bergbreiter, D. E.; and Cremer, P. S./ Specific Ion Effects on the Water Solubility of Macromolecules: PNIPAM and the Hofmeister Series. *J. Am. Chem. Soc.*, **2005**, *127* 14505-14510.

(8) Fisher, D.; and I. A. Sutherland, eds., *Separations Using Aqueous Phase Systems*, Plenum Press, New York (1989).

(9) Hatti-Kaul, R. Aqueous Two-Phase Systems. *Molec. Biothech.*, **2001**, *19*, 269-277.

(10) Zhang, H., Wang, W., Mallapragada, S., Travesset, A., Vaknin, D. Macroscopic and tunable nanoparticle superlattices. *Nanoscale* **9**, 164-171 (2017).

(11) Zhang, H., Wang, W., Mallapragada, S., Travesset, A., Vaknin, D. Ion-specific interfacial crystallization of polymer-grafted nanoparticles. *J. Phys. Chem. C* **121**, 15424-15429.

(12) Wang, W., Zhang, H., Mallapragada, S., Travesset, A., Vaknin, D. Ionic depletion at the crystalline Gibbs layer of PEG-capped gold nanoparticles brushes at aqueous surfaces. *Phys. Rev. Mater.*, **2017** *1*, 076002/1-10.

(13) Vaknin, D.; Wang, W.; Islam, F.; and Zhang. H. Polyethylene-Glycol-Mediated Self-Assembly of Magnetite Nanoparticles at the Liquid/Vapor Interface. *Adv. Mater. Interfaces*, **2018**, 1701149/1-6.

(14) Zhang, H.; Wang, W.; Akinc, M.; Mallapragada, S.; Travesset, A.; Vaknin, D. Assembling and ordering polymer-grafted nanoparticles in three dimensions. *Nanoscale* **2017**, *9* , 8710-8715.

(15) T. Ding, A. W. Rudrum, L. O. Herrmann, V. Turek, and J. J. Baumberg, Polymer-assisted self-assembly of gold nanoparticle monolayers and their dynamical switching. Nanoscale, 8, 15864-15869 (2016).

(16) B. Li, D-M. Smilgies, A. D. Price, D. L. Huber, P. G. Clem, H. Fan, Poly(N-isopropylacrylamide) Surfactant-Functionalized Responsive Silver Nanoparticles and Superlattices. *ACS-Nano*, **2014**, *8*, 4799-4804.

(17) Srivastava, S., Nykypanchuk, D., Fukuto, M., Halverson, J. D., Tkachenko, A. V., Yager, K. G., Gang, O. Two-dimensional DNA-programmable assembly of nanoparticles at liquid interfaces. *J. Am. Chem. Soc.* **136**, 8323-8332 (2014).

(18) Srivastava, S., Nykypanchuk, D., Fukuto, M., Gang, O. Tunable nanoparticle arrays at charged interfaces. *ACS Nano* **8**, 9857-9866 (2014).

(19) Wang, W., Zhang, H., Kuzmenko, I., Mallapragada, S., Vaknin, D. Assembling bare Au nanoparticles at positively charged templates. *Sci. Rep.* **6**, 26462 (2016).

(20) Zhang, H., Wang, W., Hagen, N., Kuzmenko, I., Akinc, M., Travesset, A., Mallapragada, S., Vaknin, D. Self-assembly of DNA functionalized gold nanoparticles at the liquid–vapor interface. *Adv. Mater. Interfaces* **3**, 1600180 (2016).

(21) Als-Nielsen, J., McMorrow, D. *Elements of Modern X-ray Physics*; John Wiley & Sons: England, 2011.

(22) D. Vaknin, X-ray diffraction and spectroscopic techniques for liquid surfaces and interfaces. In *Characterization of Materials*; Kaufmann, E. N., Ed.; John Wiley & Sons: New York, 2012; Vol.2, pp 1393-1423.

(23) Schlossman, M. L.; Synal, D.; Guan, Y.; Meron, M.; Shea- McCarthy, G.; Huang, Z.; Acero, A.; Williams, S. M.; Rice, S. A.; Viccaro, P. J. A Synchrotron X-Ray Liquid Surface Spectrometer. *Rev. Sci. Instrum.* **1997**, *68*, 4372-4384.

(24) Turek, V. A.; Cormier, S.; Sierra-Martin, B.; Keyser, U. F.; Ding, T.; Baumberg, J. J. The Crucial Role of Charge in Thermoresponsive-Polymer-Assisted Reversible Dis/Assembly of Gold Nanoparticles. *Adv. Optical. Mater.* **2018**, em 6,1701270/1-6

TOC Graphic

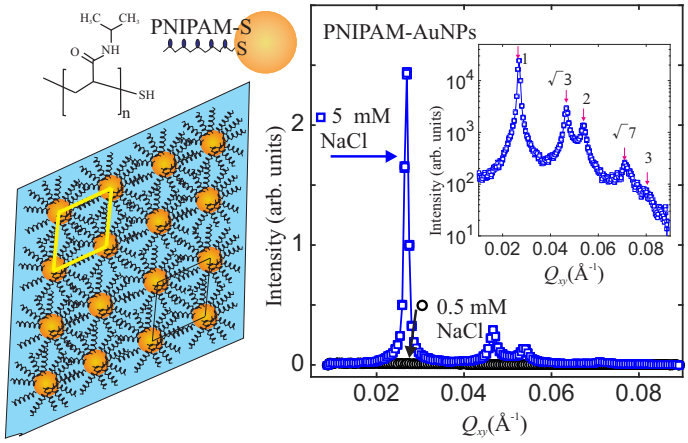
PNIPAM-S
S
PNIPAM-AuNPs
5 mM
NaCl
0.5 mM
NaCl
Intensity (arb. units)
Q_{xy}(Å^{-1})
1
√3
2
√7
3